Counter-ion binding and mobility in the presence of hydrophobic polyions – combining molecular dynamics simulations and NMR

Maksym Druchok, Natalie Malikova, Anne-Laure Rollet, Vojko Vlachy

Counter-ion binding and mobility in the presence of hydrophobic polyions – combining molecular dynamics simulations and NMR

Maksym Druchok, Natalie Malikova, Anne-Laure Rollet, and Vojko Vlachy

Citation: AIP Advances **6**, 065214 (2016); doi: 10.1063/1.4954292
View online: http://dx.doi.org/10.1063/1.4954292
View Table of Contents: http://scitation.aip.org/content/aip/journal/adva/6/6?ver=pdfcov
Published by the AIP Publishing

Counter-ion binding and mobility in the presence of hydrophobic polyions – combining molecular dynamics simulations and NMR

Maksym Druchok,[1] Natalie Malikova,[2] Anne-Laure Rollet,[2] and Vojko Vlachy[3,a]
[1]*Institute for Condensed Matter Physics, Svientsitskii 1, 79011 Lviv, Ukraine*
[2]*Sorbonne Universités, UPMC Univ Paris 06, CNRS, UMR 8234, PHENIX, F-75005, Paris, France*
[3]*Faculty of Chemistry and Chemical Technology, University of Ljubljana, Večna pot 113, SI-1000 Ljubljana, Slovenia*

(Received 16 March 2016; accepted 8 June 2016; published online 15 June 2016)

Counter-ion binding and mobility in aqueous solutions of partially hydrophobic ionene oligoions is studied here by a combination of all-atomic molecular dynamics (MD) simulations and NMR (^{19}F and ^{81}Br nuclei) measurements. We present results for 12,12–ionenes in the presence of different halide ions (F^-, Cl^-, Br^- and I^-), as well as their mixtures; the latter allowing us to probe counter-ion selectivity of these oligoions. We consolidate both structural and dynamic information, in particular simulated radial distribution functions and average residence times of counter-ions in the vicinity of ionenes and NMR data in the form of counter-ion chemical shift and self-diffusion coefficients. On one hand, previously reported enthalpy of dilution and mixing measurements show a reverse counter-ion sequence for 12,12–ionenes with respect to their less hydrophobic 3,3– and 6,6– analogues. On the other hand, the current MD and NMR data, reflecting the counter-ion binding tendencies to the ionene chain, give evidence for the same ordering as that observed by MD for 3,3–ionenes. This is not seen as a contradiction and can be rationalized on the basis of increasing chain hydrophobicity, which has different consequences for enthalpy and ion-binding. The latter is reflecting free energy changes and as such includes both enthalpic and entropic contributions. [http://dx.doi.org/10.1063/1.4954292]

I. INTRODUCTION

Understanding polyelectrolyte solutions is of importance for basic sciences, most notably for chemistry and biology, as well as, for various technologies.[1–5] In last decades we witness a revival of interest in polyelectrolyte studies, resulting in new materials and applications, ranging from electronics to medicine (see for example Refs. 6–8). One reason for the growing interest is the fact that most polyelectrolytes are soluble in water and can therefore be applied in aqueous media. This is important for it makes them compatible with physiological systems and also because of environmental concerns. Further increase in polyelectrolyte applications is only possible if deeper understanding of the structure and properties of these complex solutions can be obtained.

An important subgroup of polyelectrolytes in which the ionic groups form part of the polymer backbone are so-called ionenes.[9–15] In recent years we extensively studied aliphatic ionenes, i.e. the cationic polyelectrolytes, with the repeating unit "–[$^+$N(CH$_3$)$_2$ – (CH$_2$)$_x$ –$^+$N(CH$_3$)$_2$ – (CH$_2$)$_y$]–", where integers x and y denote the number of methylene groups between the adjacent nitrogen

[a]Author to whom correspondence should be addressed. Electronic mail: vojko.vlachy@fkkt.uni-lj.si

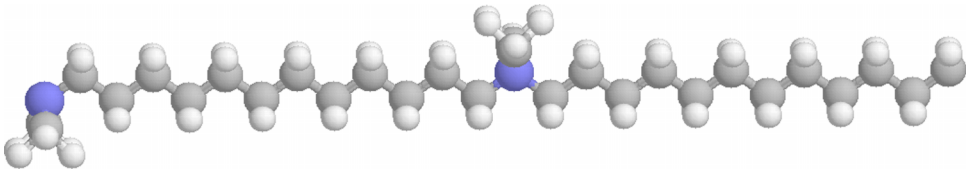

FIG. 1. Schematic (fully extended) representation of two repeating units of the 12,12–ionene polyion ($x = y = 12$). One quaternary ammonium group (nitrogen in blue, carbons in grey and hydrogens are in white color) is followed by twelve methylene groups. Together they form the polyion backbone. Methyl groups are located on nitrogens and as such stretch into the solvent.

atoms (Figure 1 illustrates 12, 12–ionene fragment). Experimental studies have been performed for x, y equal to 3,3–, 4,5–, 6,6–, and 6,9– to 12,12–ionenes, that is for increasingly more hydrophobic polyelectrolytes.[16–23] Among physico–chemical properties we measured enthalpies of dilution and mixing, osmotic coefficients, dielectric relaxation, conductivities and transport numbers. These solutions have also been examined using NMR, X-ray and neutron scattering methods.[24,25] Experimental studies were accompanied by molecular dynamics (MD) simulations.[17,26–29]

The experimental results mentioned above indicate strong deviations from theoretical predictions based on the classical theories of polyelectrolyte solutions.[16,18,19,21,22,25] We mention now in more detail the enthalpies of dilution and mixing, notice that both quantities provide similar physical information, but they carry an opposite sign. For example, the enthalpy of dilution ΔH_{dil} is on the basis of the electrostatic theory[30] expected to be exothermic but experiments prove that ΔH_{dil} can also be positive. The discrepancies between theory and experiments vary with the charge density of the poly-cation and the nature of counter-ions and/or salt present in solution. Enthalpies of dilution and ionene–salt mixing, ΔH_m, revealed correlation with the enthalpy of hydration of the counter-ion species, ΔH_{hyd}. More precisely, the enthalpy of mixing of 3, 3–ionene (and of 6, 6–ionene) fluorides with sodium halides can be expressed as a linear function of the enthalpy of hydration, ΔH_{hyd}, of the halide counter-ions. The sequence follows the direct Hofmeister series (see Figure 5 of Ref. 17): ΔH_m is mostly negative and decreases in the order $F^- > Cl^- > Br^- > I^-$. Similarly to the above sequence, the counter-ion trends concerning the strength of counter-ion binding to the ionene oligoion, observed in experimental[22,23] and MD simulation data,[17,26–29] were: F^- (weakest binding) $< Cl^- < Br^- < I^-$ (strongest binding). Very interestingly, the calorimetric (ΔH_m and ΔH_{dil}) data for 12, 12–ionenes, presented in our recent study[21] did not follow the above trends. Upon titration of 12, 12–ionene fluoride solutions with NaBr the effect was endothermic ($\Delta H_m > 0$) – quite the opposite to the less hydrophobic 3, 3– and 6, 6–ionene solutions (see Figures 3 and 4 of Ref. 21), where it was exothermic. Further the ΔH_{dil} of 12, 12–ionene bromide solutions was more negative than for 12, 12–ionene fluoride, which again was opposite to the previous findings for more charged (3, 3– and 6, 6–) ionenes dissolved in water. Beside the different enthalpic trends, we have equally reported a difference in ionene chain conformation as seen through effective chain-chain interactions probed by neutron scattering. We observed structural changes between 12,12-ionenes and their more strongly charged analogues and linked this to the emerging signature of chain hydrophobicity.[25] Are these changes reflected also in the counter-ion binding tendencies of strongly and weakly charged ionenes? That is the question the current contribution tries to answer, by probing ion-binding through MD and NMR.

The present study complements our previous theoretical and experimental results for aliphatic ionene solutions in water.[17,18,21] Here we compare properties of the most hydrophobic ionenes (12, 12–ionenes) studied so far with their less hydrophobic analogues (3, 3– and 6, 6–ionenes). We employ a combined approach of molecular dynamics simulation and NMR (^{19}F and ^{81}Br nuclei) spectroscopy. Special attention is paid to the nature of counter-ions and their binding competition to ionene chains in aqueous solutions. We consolidate both structural and dynamic information, in particular radial distribution functions and average residence times in the vicinity of 12, 12–ionenes obtained by simulation on one hand, chemical shift and counter-ion self-diffusion coefficients measured by NMR on the other.

TABLE I. Model parameters: equilibrium bond distances r_0 and angles θ_0 governing the ionene intramolecular structure.

ionene carbon chain	r_0 (N-C)	1.5 Å
	r_0 (C-C)	1.5 Å
	θ_0 (N-C-C)	111°
	θ_0 (C-N-C)	111°
	θ_0 (C-C-C)	111°
CH_3- and CH_2- groups	r_0 (C-H)	1.1 Å
	θ_0 (H-C-H)	108°

The study of ionenes or other synthetic polyelectrolytes of increasing hydrophobicity has a wider importance. Such systems can serve as models for more complicated biological molecules, such as proteins or nucleic acids, which contain both charged and non-polar groups. This may modify the solvation of embedded charges and influence the potential of mean force between the macromolecules and ions in solution.[21,31]

II. SIMULATION AND EXPERIMENTAL DETAILS

Molecular dynamics simulations were performed using the standard DL_POLY package.[32] The unit cell contained four 12, 12–ionene polyions, sixteen counter-ions (F^-, Cl^-, Br^-, or I^-), and 6300 water molecules. The ionene monomer concentration was the same as for previous MD studies of 3, 3– and 6, 6–ionene solutions;[17,26,28,29] $c(N^+) = 0.14$ mol/dm^3. No additional salt (no co-ions) was present in the system. Simulations were also performed for mixed counter-ion solutions with F^-/Br^- ratio equal to 1:1. The latter simulations allowed us to probe the preferential binding of counter-ion species to polyion; ion–binding accompanied with the desolvation effect appeared to be at least partly responsible for the previously reported ion–specific effects for ionenes.[16–19]

The 12, 12–ionene oligoions were represented by four quaternary nitrogen centers joined by three segments of twelve methylene (CH_2) groups. This means that the model ionene has a somewhat higher charge density than the real one, where the end effects are negligible. In order to preserve ionene internal geometry we used additional conditions for bond lengths and valence angles (see Table I) in the form of: $E_{bond}(r) \sim (r - r_0)^2$ and $E_{angle}(\theta) \sim (\theta - \theta_0)^2$. The charges ($Z_i$) and the Lennard–Jones parameters (σ_i, ϵ_i) assigned to the various atoms, listed in Table II, were the same as in Refs. 17 and 26–29. The Lennard–Jones parameters for ionene particles were taken from the OPLS force field[33] and the parameters for halide ions from Ref. 34. We modeled water using the SPC/E model.[35] For unlike sites the Lennard–Jones parameters were obtained via the

TABLE II. Model parameters: charges (Z_i) and the Lennard–Jones parameters (ϵ_i, σ_i). Carbon atoms in –CH_3 groups are denoted by C1, carbon atoms in –CH_2 by C, hydrogen atoms in –CH_2 and –CH_3 groups neighboring the nitrogen by H2, and hydrogen atoms in –CH_2 groups of the alkyl chain by H1. e_0 is the elementary charge.

species	atom or ion (i)	Z_i / e_0	ϵ_i / kcal mol^{-1}	σ_i / Å
water	O	−0.8476	0.1554	3.1656
	H	0.4238	0.0	0.0
ionene	N	0.60	0.170	3.25
	C	−0.20	0.066	3.50
	C1	−0.25	0.066	3.50
	H1	0.10	0.030	2.5
	H2	0.13	0.030	2.5
ions	F	−1.00	0.0118	4.0
	Cl	−1.00	0.0403	4.86
	Br	−1.00	0.0645	5.04
	I	−1.00	0.0979	5.40

Lorentz–Berthelot combining rules. All the species were allowed to move freely across the unit cell of size 58 Å × 58 Å × 58 Å. The Ewald summation technique was used to account for the long–range Coulomb interactions. We applied the N,P,T ensemble with the pressure (1 bar) and temperature (298 K) controlled by the Nose–Hoover barostat and thermostat.[36] The cut-off distance for the short-range interactions was 15 Å. We used the leapfrog algorithm to integrate the equations of motion with a time step of 0.5 fs. The length of the production runs ranged from 11 to 12 ns. For the sake of comparison we also performed new simulations of the 3,3–ionene solution with F^- and Br^- counter-ions present in the 1:1 ratio (no additional salt present). The system consisted of 2352 water molecules, one 3,3–ionene molecule with six nitrogen sites and six neutralizing counter-ions. The unit cell had a size 42 Å × 42 Å × 42 Å and the production run lasted 50 ns. Other simulation details were the same as for the 12,12–ionene case.

Single pulse ^{19}F NMR spectra were recorded using a Bruker Avance III 300 MHz NB spectrometer, operating at 7.05 T. All samples were ionene solutions in light water (H_2O) and the lock was obtained with a sealed 2.5 mm capillary filled with D_2O inserted into the NMR tube. The chemical shift was referenced to $CFCl_3$. Pulsed field gradient NMR (PFG-NMR) experiments were performed using a BBFO probe equipped with 55 Gauss/cm gradient coil. We used a NMR pulse sequence combining bipolar gradient pulses and stimulated echo.[37] This sequence was repeated with 16 gradients of increasing strength ($0<g<50$ Gauss/cm, gradient application time of 1.5 ms) and a diffusion time of 100 ms. The self-diffusion coefficients were obtained by nonlinear least-square fitting of the echo attenuation. ^{81}Br spectra were equally recorded with a Bruker Avance III 300 MHz spectrometer. Due to the high NMR relaxation rate of the ^{81}Br nucleus, its spectrum is significantly distorted by the ringing (electronic and/or electroacoustic) of the probe.[38,39] In order to overcome this problem we have used a composite pulse sequence,[40,41] with a 90 degree pulse of 10 μs and a recycling delay of 200 ms. The number of scans ranged from 2048 to 8192 depending on the sample. The spectra were fitted using DMFIT software.[42]

III. RESULTS AND DISCUSSION

A. Molecular dynamics results

First, in Figure 2 we consider hydration of nitrogen atoms, where the positive charge on the ionene molecule resides. The influence of different halide counter-ions on the water oxygen–nitrogen radial distribution function (RDF) is examined. The results for F^- ions are shown by red continuous line, for Cl^- ions with green dashed and Br^- blue dotted lines, and for I^- by dotted magenta lines. Ionenes of three different charge densities are probed: the 12,12–ionene results are shown on panel (a), the 6,6– on panel (b), and 3,3–ionene functions on panel (c). Notice that 6,6– and 3,3–ionene RDFs were collected during the MD simulations presented in Ref. 29 but have not been published so far.

As we see the resulting radial distribution functions are sensitive to the linear charge density of the ionene studied, while the differences between the counter-ions studied here are very small. Notice again that x, y–ionene oligoions differ from each other in the length of the unit carrying one elementary charge. The spacings between two positive charges vary from three ($x = y = 3$) to twelve CH_2 units ($x = y = 12$) for 12,12–ionene (see Figure 1 and comment on the 12,12–ionene model in Section *Simulation and experimental details*). The charge density of the polyion strongly affects the thermodynamic and transport properties of polyelectrolyte solutions.[18,19,21] The consequence of higher accumulation of positive charge on the 3,3–ionenes in comparison with less charged 6,6– and 12,12–ionenes is reflected in the relevant RDFs. For 3,3 ionenes the water oxygen–nitrogen RDF exhibits a small shoulder approximately at 4.3 Å, which is due increased probability of finding water molecules in the domain between two adjacent nitrogen atoms. This is confirmed by the water oxygen–carbon(CH_2) distribution function (not shown here), having a peak around 3.6 Å. Yet another consequence of high linear charge density of the 3,3– ionenes is the fact that water ordering extends to large distances. This is implied by strong second and noticeable third peak in the RDF. The results are consistent with the counter-ion distributions shown later in panel (b) of Figure 5.

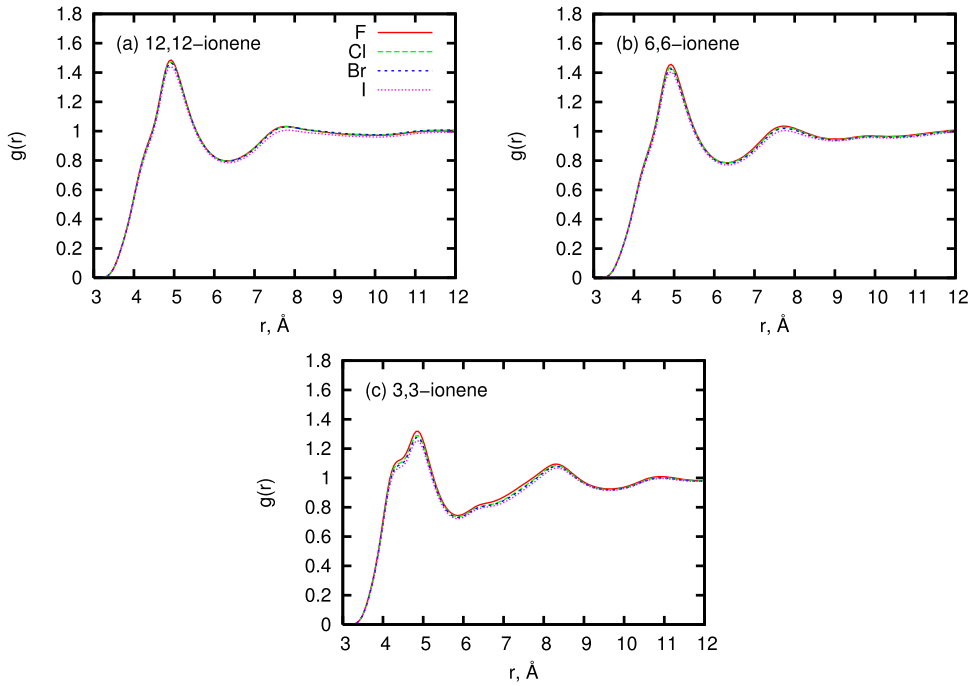

FIG. 2. The water oxygen–nitrogen RDFs for x, y–ionene solutions. In panel (a) we show the results for 12, 12–ionenes, in panel (b) the data for 6, 6–, in panel (c) results for 3, 3–ionenes. The solutions with F counter-ions are denoted by red red solid, those with Cl by green dashed, Br by blue dotted, and those with I counter-ion by magenta dotted line.

In Figure 3 we present the nitrogen–counter-ion radial distribution functions. Similarly to the less hydrophobic ionenes, the I^- counter-ions exhibit a high peak in the proximity of the positive charge, while F^- ions are distributed more evenly throughout the volume.[29] Due to the lower charge density on 12,12–ionenes, the peaks in the proximity of the oligoions are less pronounced in comparison with their 3, 3– and 6, 6– analogues. Experimental results for the heats of dilution and heats of mixing as well as previous MD simulations (see for example Ref. 28) suggest that I^- ion is losing some of the hydration water when interacting with ionene molecules. On the other hand F^- ions hold their waters tightly, which hinders the association between F^- ions and the charged nitrogen atom. The distribution of F^- is, except in the region close to the oligoion in which ions cannot penetrate, more or less uniform. The coordination numbers of water oxygens around various counter-ions approaching the nitrogen centre on the 3, 3–ionene are presented in Figure 10 of Ref. 27 and for 6,6–ionenes in Figure 3 of Ref. 28. While the Cl^-, Br^-, and I^- ions

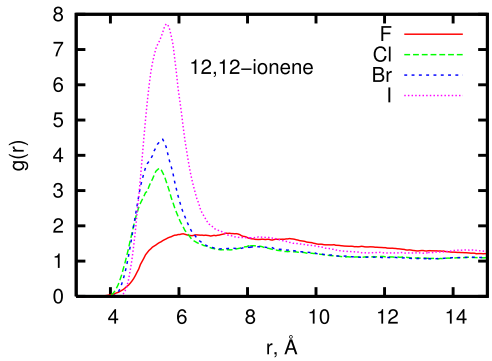

FIG. 3. The nitrogen–counter-ion RDFs for 12, 12–ionenes. The N-F counter-ions RDF is denoted by red solid, N-Cl – by green dashed, N-Br – by blue dotted, and N-I counter-ion RDF by magenta dotted line.

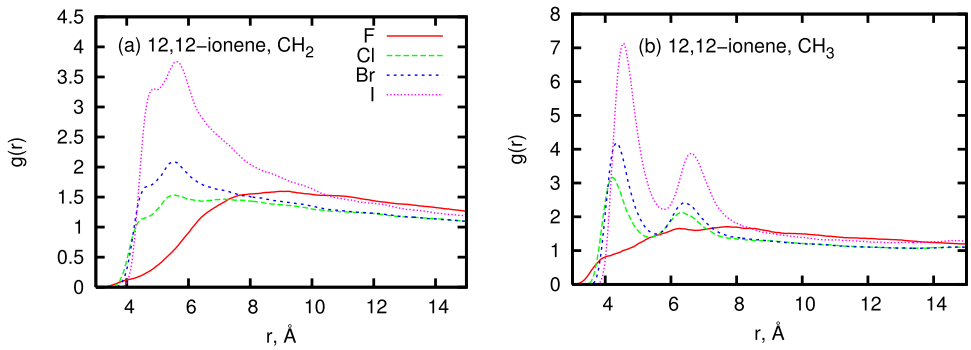

FIG. 4. The carbon–counter-ion RDFs for 12, 12–ionenes. Panel (a) shows the counter-ion distributions around carbons in CH_2 groups and panel (b) the same for CH_3 groups. The C-F counter-ion RDF is denoted by red solid, C-Cl – by green dashed, C-Br – by blue dotted, and C-I counter-ion RDF by magenta dotted line. The differences in the RDFs of two groups are the consequence of their different sizes and positions. While CH_2 groups are forming the backbone of the oligoion, the bulkier CH_3 groups are side groups located on the nitrogen atoms and are more exposed.

lose some of the hydration shell water when approaching the positive charge, this not the case for F^- counter-ions, which keeps its hydration shell intact. Fluoride ion has, namely, more negative free energy of hydration than the other ions mentioned above. The radial distribution functions for counter-ions around carbon atoms are given in Fig. 4. We distinguish two different classes of carbon atoms: those on the main backbone (denoted by C, panel (a) of Fig. 4) and those belonging to the methyl groups (C1; panel (b)). The ion–specific effects are clearly visible also here – the RDF peak for I^- counter-ion is much higher than for the other ionic species. The differences between the CH_2 and CH_3 groups come mostly from their positions on the ionene oligoion. While CH_2 groups are forming the backbone of the oligoion, the bulkier CH_3 groups are side groups located on the nitrogen atoms and are more exposed. In this way there are more accessible for water and counter-ions than CH_2 groups.

The results for 12, 12–ionene and 3,3–ionene oligoions in water, neutralized with two counter-ion species (F^-/Br^- mixture in the 1:1 ratio) are shown in Figure 5. On this figure we present N–F and N–Br radial distribution functions for 12, 12–ionenes (panel a) and for 3, 3–ionenes (panel b). The RDFs for pure 3,3–ionene fluorides (green dashed line) and bromides (magenta dotted lines) were presented in Ref. 29 and are for the sake of easier visualization of the charge density effect shown again. These results demonstrate how the radial distribution functions between nitrogen atom and a given counter-ion modifies, when moving from a homo-ionic to a mixed-ionic solution. Due to smaller numbers of ions of each species in the simulation box, these RDFs are given with larger uncertainties than those shown in previous figures.

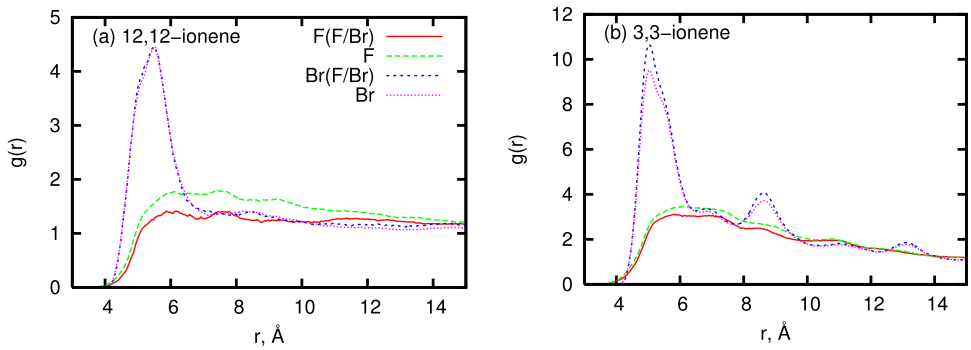

FIG. 5. The RDFs for F^- and Br^- counter-ions around the nitrogen of 12, 12–ionenes (panel (a)) and of 3,3–ionenes (panel (b)): N–F in mixed counter-ion (F^-/Br^-) systems (red solid lines), N–F in pure F^- systems (green dashed lines), N–Br in mixed counter-ion (F^-/Br^-) systems (blue dotted lines) and N–Br in pure Br^- systems (magenta dotted lines).

For 12, 12–ionenes the N–Br radial distribution function is practically unaffected when we replace some Br^- by F^-. The opposite is not true: the distribution of F^- ions is suppressed in the vicinity of the oligoion, when we replace some F^- by Br^-. A similar conclusion, notice the difference in scales, can be drawn for N–F RDF obtained for 3, 3–ionenes (panel b), but here the effect is accompanied by an increase of the N–Br distribution function when we pass into the ion mixture. The results are consistent with simulations of "pure" counter-ion–ionene solutions, where a stronger binding of Br^- ions is observed in comparison with F^- ions.

B. Residence times and fractions of "free" counter-ions

We are interested in degree of "binding" of various counter-ion species to the 12, 12–ionene oligoions. In the spirit of our previous study,[29] we first define the domains around the relevant atoms on the ionene. The counter-ion is considered to be visiting (it is "bound" to) a particular atom when its center is lying within a pre–defined spherical domain centered on the atom. The radii of these domains are taken to be equal to distances from origin to first minima of the corresponding RDFs (N–X, C–X, C1–X), shown in Figs. 3 and 4. This criterion is not applicable to F^- ions because the F–ionene RDFs have no distinct first minimum. This problem was noticed before[29] and, for the sake of comparison with other counter-ion species, the domain radii for F^- ions were chosen to be equal to those of the Br^- ion. We use the same prescription here. Notice, that the size of the characteristic radius, within which the particular counter-ion species contributes to the residence time, depends not only on the nature of the counter-ion but also on the type of the ionene studied. The sizes of radii, defining the domains for 12, 12–ionenes, are shown in Table III.

The protocol to evaluate the residence times and build the corresponding distribution consists of the following steps: (i) during the simulation we analyze instantaneous configurations and identify the counter-ions residing within a domain of interest, (ii) we repeat this step periodically (every 5 simulations steps, that is on 2.5 fs interval), (iii) if the counter-ion remains within the domain area, the corresponding "stopwatch" keeps running, otherwise iv) the residence time distribution is updated and the "stopwatch" zeroed. Some authors suggested to use the so-called "wait" or "tolerance" time in order to exclude the unsuccessful exchange ("in-and-out" attempts).[43,44] Unfortunately, the value of tolerance time has to be set arbitrarily and different choices of it may yield different interpretations of the simulation results.[44] To avoid this problem we present the results as they follow directly from simulations.

We examine the residence time distribution $f_1(\tau)$, where τ is a duration of a counter-ion visit to the domain $\Omega_N \bigcup \Omega_C \bigcup \Omega_{C1}$ (ionene as whole). The counter-ion is considered to be contributing to this distribution if the distance to a nearest nitrogen or carbon (C and C1) atom of the oligoion remains less than the introduced radius (Table III). Otherwise the counter-ion is out of this domain and it does not contribute to $f_1(\tau)$. According to this definition, counter-ions stay within the oligoion domain if they travel along the ionene chain, but loose the correlation if they depart from an oligoion in the radial direction. In addition to $f_1(\tau)$, we also define he probability density $f_2(\tau)$. Here τ is a duration of a counter-ion visit to the domain centered on a nitrogen atom. Every Ω_N domain consists of only one nitrogen. The number of Ω_N domains is therefore equal to the number of nitrogens in the system. The jumps (in 12, 12–ionene case not very probable) between different nitrogens are considered as separate visits. Accordingly, $f_2(\tau)$ measures the distribution of the residence time to the domain Ω_N around nitrogen atoms. The same characteristic N–X distances

TABLE III. Characteristic radii r_i (in Å) within which fluoride, chloride, bromide, and iodide counter-ions contribute to the residence times, τ, for 12, 12–ionenes. Within the spherical domains, defined by these radii, the counter-ions are assumed to be "bound" to the particular atom.

ionene-site	r_F	r_{Cl}	r_{Br}	r_I
N	7.2	7.2	7.2	7.7
C	4.7	4.6	4.7	4.9
C1	5.6	5.4	5.6	5.8

TABLE IV. The histogram $H_1(\tau_a;\tau_b)$ defined in Eq. (1), the domain of interest is $\Omega_N \bigcup \Omega_C \bigcup \Omega_{C1}$.

	$H_1(\tau_a;\tau_b)$			
Time domain (ps)	F	Cl	Br	I
0–1	0.905	0.878	0.878	0.860
1–2	0.040	0.046	0.050	0.060
2–5	0.026	0.028	0.029	0.031
5–10	0.012	0.015	0.013	0.012
10–20	0.009	0.015	0.014	0.011
20–30	0.004	0.008	0.007	0.007
30–50	0.003	0.006	0.007	0.009
50–125	0.001	0.004	0.004	0.011

as above apply. Notice, that in this case the counter-ion can loose its correlation with the nitrogen on the oligoion either by moving in a radial direction (away from the ionene) or traveling along the oligoion chain.

For completeness and to allow comparison with previous study[29] we constructed histograms showing time in picoseconds spent by the counter-ion in the domains of interest. The distributions are pooled into time intervals from 0–1 ps, 1–2 ps, 2–5 ps, 5–10 ps, 10–20 ps, 20–30 ps, and 30–50 ps, and 50–τ_{max} ps, as suggested by Eq. (1)

$$H_i(\tau_a;\tau_b) = \frac{\int_{\tau_a}^{\tau_b} f_i(\tau)\mathrm{d}\tau}{\int_0^{\tau_{\max}} f_i(\tau)\mathrm{d}\tau}. \tag{1}$$

The limiting value τ_{max} = 125 ps was chosen on the basis of observation – no visits longer than 125 ps were seen. The results presented in Tables IV and V indicate, in agreement with previous calculations for 3,3– and 6,6–ionenes,[29] that a great majority of the visits lasts less than 1 ps. Also, there are some differences in histograms depending on the nature of the counter-ion; fluoride ions exchange on a faster rate than the other three ions. This has been observed before.[29] Interestingly, there is little difference between the two distributions (compare Tables IV and V), much less than that found for the 3,3–ionenes.[29] Because the sizes of the domains vary from 3,3– to 12,12–ionenes a more quantitative comparison of the $H_i(\tau_a;\tau_b)$ distributions for various ionenes is not possible.

From the distributions, $f_i(\tau)$, we can also calculate the average residence times in the particular domains (i):

$$\langle\tau\rangle_i = \frac{\int_0^{\tau_{\max}} \tau f_i(\tau)\mathrm{d}\tau}{\int_0^{\tau_{\max}} f_i(\tau)\mathrm{d}\tau}, \tag{2}$$

The results for the average residence times of counter-ions for "pure" and "mixed" counter-ion systems are listed in Table VI. The average residence times, $\langle\tau\rangle_i$, defined above, increase from F^-

TABLE V. The histogram $H_2(\tau_a;\tau_b)$ defined in Eq. (1), the domain of interest is Ω_N.

	$H_2(\tau_a;\tau_b)$			
Time domain (ps)	F	Cl	Br	I
0–1	0.906	0.860	0.856	0.856
1–2	0.040	0.048	0.051	0.055
2–5	0.027	0.035	0.036	0.037
5–10	0.012	0.020	0.019	0.016
10–20	0.008	0.019	0.018	0.013
20–30	0.004	0.008	0.008	0.007
30–50	0.002	0.006	0.008	0.009
50–125	<0.001	0.003	0.004	0.007

TABLE VI. Average residence times $\langle\tau\rangle_i$ in picoseconds (ps), for 12,12-ionenes. The last two columns apply to F^-/Br^- mixed counter-ion case. Numerical uncertainty of this quantity is estimated to be ±5 %.

	F	Cl	Br	I	F (F/Br)	Br (F/Br)
ionene, $\langle\tau\rangle_1/ps$	0.76	1.33	1.31	1.98	0.73	1.34
nitrogen, $\langle\tau\rangle_2/ps$	0.66	1.36	1.46	1.66	0.68	1.53

to I^- counter-ion. This holds true (within the uncertainty of simulations) for both the "ionene", $\langle\tau\rangle_1$, and the "nitrogen" domain, $\langle\tau\rangle_2$. We have already seen such trends for 3,3– and 6,6–ionenes.[29]

For Br^- counter-ions $\langle\tau\rangle_1$ is less than $\langle\tau\rangle_2$. One would expect an opposite behavior, $\langle\tau\rangle_1 \geq \langle\tau\rangle_2$, because the ionene domain is larger than the nitrogen one. The larger domain allows more moves along the ionene chain and, in principle, longer residence times. The shorter average times for larger domains is a consequence of many short–time visits to the non–polar parts of ionene molecule, decreasing the overall $\langle\tau\rangle_1$ time. The average time for Br^- ions in the F^-/Br^- mixture slightly increases, but the effect is within the numerical uncertainty and, accordingly, no firm conclusions can be made.

Fractions of "free" counter-ions can be either calculated during the simulations directly or, alternatively, from the residence time distributions $f_i(\tau)$:

$$\alpha_i = 1 - \frac{1}{N_c \overline{T}} \int_0^{\tau_{\max}} \tau f_i(\tau) d\tau \tag{3}$$

where N_c is the number of counter-ions in the system, and $\overline{T}$ is the total simulation time. Both, Eq. (3) and the direct averaging yielded the results which agree within ±5 %. We take this estimate as a measure of the numerical accuracy of the residence times and α_i calculations. The differences in fractions α_i between the two domains are within the uncertainties of simulations. The results are summarized in Table VII.

For homoionic 12,12–ionenes, the simulation results (Table VII) indicate a much higher fraction of "free" counter-ions in case of F^- than in case of I^- counter-ions, as observed for more charged ionenes. The differences in results between the "nitrogen" and "ionene" domains are within the uncertainties of simulations. The comparison of results in Table VII with those in Tables IX and X of Ref. 29 somewhat surprisingly indicates that the fraction of free counter-ions is for most ions larger for the 6,6– than for the 12,12–ionene oligoions. Notice, however, that in the latter case the radius of the domain within which the ions are considered "bound" is larger.

For the ionene solutions neutralized by a single counter-ion species the fractions of "free" counter-ions were measured by Rodič et al.[22] They applied a combination of conductivity and transport number measurements to determine this quantity in solutions of 3,3–, 6,6– and 6,9–ionenes. The solutions with F^- and Br^- counter-ions were probed at 298 K. It was found that binding of counter-ions to the polyion, in addition to the charge density of the latter, depends also on the chemical nature of the counter-ion in question. The experimentally determined fraction of "free" F^- ions is for 3,3–ionene solutions distinctly higher than those of Br^- counter-ions. The same trend is observed for 6,6– and 6,9–ionenes, but in the latter case, the difference in ion–binding between the two ionic species is within the experimental error. In yet another study,[23] we used calorimetric data to perform a model thermodynamic analysis of the polyelectrolyte–salt mixing

TABLE VII. Fraction of "free" counter-ions α_i, for 12,12–ionenes. The last two columns are for F^-/Br^- mixed counter-ion case. Numerical uncertainty of this quantity is estimated to be ±5 %.

	F	Cl	Br	I	F (F^-/Br^-)	Br (F^-/Br^-)
ionene, $\alpha_1/\%$	85.0	78.5	76.0	58.0	90.0	76.5
nitrogen, $\alpha_2/\%$	85.5	79.5	78.0	61.0	90.0	78.5

process. The results prove that halide ions replace F^- counter-ions with a strength increasing in the order $Cl^- < Br^- < I^-$.

Variations in the binding ability of different counter-ions to ionene chains should yield a "selectivity", to be observed in systems with several simultaneously present counter-ions. The last columns in Table VII suggest a higher fraction of "free" F^- ions as opposed to Br^- ions in mixed counter-ion 12, 12–ionenes. This finding agrees well with our conclusions for ionenes with only one counter-ion species neutralizing the ionene. In the "mixed" F^-/Br^- counter-ion case, the fraction of "free" F^- ions grows at the expense of Br^- counter-ions, the former being less successful in the "binding competition". In other words, Br^- ions push some F^- ions toward the bulk of solution, to increase the population of "free" counter-ions. The results reflect the fact that Br^- ions do not keep their hydration shell as strongly as F^- ions;[28] their hydration free energy is less negative (see, for example, Ref. 45). This also explains why in the mixed systems average residence times of Br^- increase (and the corresponding times for F^- decrease) in comparison to their homo-ionic analogues (see Table VI).

At the end we wish to stress that average residence time does not contain the same information as fraction of bound counter-ions.[29] This is because various $\langle\tau\rangle_i$ do not provide an information about the overall time that a particular counter-ion spends in the domain of interest. The same fraction of bound counter-ions can be obtained as a result of many short visits or, alternatively, fewer but longer visits of the counter-ion to the domain of interest.

C. Binding of counter-ions as seen by the NMR experiments

For selected nuclei, NMR measurements are very well adapted to probe the anion binding competition in ionene solutions[46] and, in particular, in the case of ionene solutions with mixed counter-ion clouds. We present here the results from ^{19}F and ^{81}Br NMR measurements. For the dipolar ^{19}F nuclei, both chemical shifts and self–diffusion coefficients were measured, while for the quadrupolar ^{81}Br nuclei we focused on the full width half maximum (FWHM) of the NMR peak. Due to the fast relaxation of the ^{81}Br nuclei, measurement of the self–diffusion coefficient is not possible. Note that the characteristic length and time-scales of our MD and NMR measurements are too far apart for a direct comparison between MD and NMR quantities and it was not our goal. We can however compare and comment upon the ion-binding trends that stem from the interpretation of MD and NMR data and that is the approach here.

Our recent NMR measurements performed on 3, 3–ionenes with a mixture of F^- and Br^- counter-ions,[25] confirm the above–mentioned picture of the binding competition between strongly and weakly hydrated anions. Interestingly, NMR results for 12, 12–ionenes show a different behaviour to 3, 3–ionenes. Figure 6 compares the chemical shift of the ^{19}F nuclei, $^{19F}\delta$, as well as the self–diffusion coefficients, $D(^{19}F)$, between the two systems. The molar fraction of Br^- counter-ions (x_{Br}) ranges from 0 to 0.8 along each series, as indicated in the figure. Figure 6 features three series of mixed Br/F ionenes with different volume fractions occupied by the ionene, ϕ, and overall charge concentration in the solution, $c(N^+)$: (a) 3, 3–ionenes at $c(N^+)$=1 M, $\phi = 0.10$, (b) 3, 3–ionenes at $c(N^+) = 0.2$ M, $\phi = 0.02$ and (c) 12, 12–ionenes at $c(N^+) = 0.3$ M, $\phi = 0.07$. The comparison between the three series is instructive, as series (a) and (c) are close in the volume fraction (ϕ) but possess different $c(N^+)$, while series (b) and (c) are close in $c(N^+)$ but have different volume fraction (ϕ).

The chemical shift is sensitive to the very neighbourhood of the probed nucleus, i.e. the first shells of neighbours. As shown in Figure 6 (left), for the ^{19}F nucleus no significant variation of its chemical shift ($^{19F}\delta$) is observed as a function of x_{Br}, in the case of 12,12–ionenes (series c). It means that whatever the x_{Br}, the lowly charged 12,12–ionene chain provides a weak perturbation to the local magnetic field of the F^- nuclei present. This trend contrasts with that observed for 3,3–ionenes (series a), for which this perturbation is stronger (chemical shift is further away from the 1 M NaF reference value of −119.798 ppm) and, in addition, the shift is sensitive to the composition of the counter-ion atmosphere (represented by x_{Br}). With increasing fraction of Br^- counter-ions, $^{19F}\delta$ moves to more negative values, in the direction of the NaF reference value. This

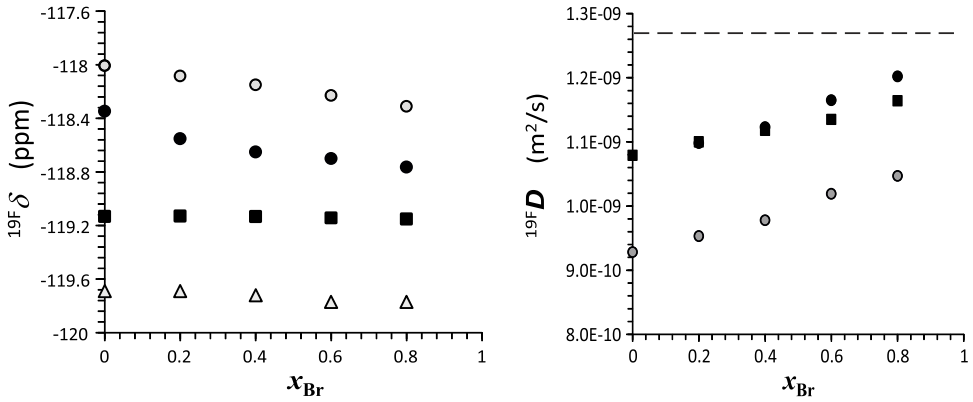

FIG. 6. ^{19}F NMR data for three series of mixed F^-/Br^- ionenes, with different volume fractions occupied by the ionene, ϕ, and varying the overall charge concentration in the solution, $c(N^+)$: 3,3–ionenes at $c(N^+)$= 1 M, $\phi = 0.10$ (series a, grey circles), 3,3–ionenes at $c(N^+) = 0.2$ M, $\phi = 0.02$ (series b, black circles) and 12,12–ionenes at $c(N^+) = 0.3$ M, $\phi = 0.07$ (series c, black squares). Molar fraction of Br^- counter-ions (x_{Br})ranges from 0 to 0.8 along each series. Left panel features the chemical shift of the ^{19}F nuclei, $^{19F}\delta$, in the three ionene series, as well as data for F^-/Br^- reference at $c(N^+)$=1 M (grey triangles). Right panel features the corresponding self-diffusion coefficients, $D(^{19}F)$. The value of $D(^{19}F)$ for 1 M NaF solution is represented by a horizontal line. The error bar is smaller than symbol sizes.

points clearly towards a preferential displacement of F^- by Br^- in the vicinity of the 3,3–ionene backbone, as the proportion of the latter increases.[25]

Overall, decreasing the linear charge density of the ionene backbone (passage from 3,3– to 12,12–), but maintaining the same volume fraction occupied by the ionene, yields $^{19F}\delta$ which is insensitive to the proportion of Br^- and F^- ions. Moving towards the diluted 3,3–ionene (series b), we maintain the same (low) overall charge concentration as for series c, but we impose again the narrow spacing of charges on the ionene backbone. The significant variation of $^{19F}\delta$ as a function of x_{Br} is recovered. The high linear charge density on the ionene backbone (and thus a dense counter-ion atmosphere) seems necessary to induce significant changes in the chemical shift of the F^- as these ions are displaced by Br^- and this *irrespective* of the ionene volume fraction in the solution.

The self–diffusion coefficients of F^- ions, $D(^{19}F)$, in the above three systems are shown in Figure 6 (right) and are seen to increase with an increase of x_{Br} in all cases, towards the reference value in 1 M NaF aqueous solution, which is 1.265×10^{-9} m^2s^{-1}. It is important to note that the presented measurements of the diffusion coefficient using pulsed field gradient NMR correspond to a lengthscale of μm and a timescale of ms. On this scale, the probed nucleus explores repeatedly both "bound" and "free" states and the resulting value is an average over these environments. The rise of $D(^{19}F)$ with an increase of x_{Br} is thus interpreted as an increasing probability for F^- ions to be present in the domain away from the ionene backbone (i.e. in the "free" state). As such, the F^- ions closer to the backbone are gradually expelled by Br^- ions, which occupy these states preferentially. For 3,3–ionenes, it is clear that trends shown by both the chemical shift and the self-diffusion coefficients of F^- ions can be explained on the basis of this picture. For 12,12–ionenes, we lose the sensitivity of the chemical shift to x_{Br}, but retain sensitivity to x_{Br} in the diffusion coefficient. This does not however contradict the proposed picture of F-Br competition in the vicinity of the backbone and it can still be applied to 12,12–ionenes. We cannot assume the same sensitivity of the two quantities to x_{Br}. Chemical shift for dipolar nuclei (case of ^{19}F) is only sensitive to the perturbation of the magnetic field on a very local scale (within a few Å), while the self-diffusion coefficient is sensitive to a wider environment, being influenced by the interactions with the polyelectrolyte backbone, changes in the hydration shell etc.

We can further discuss the relative values of $D(^{19}F)$ for the three data sets. For the concentrated 3,3–ionene solution, the diffusion coefficient is most significantly diminished with respect to the reference value. Both the high charge density on the backbone and the high ionene volume fraction contribute to this. Decreasing the ionene volume fraction or decreasing the backbone charge density

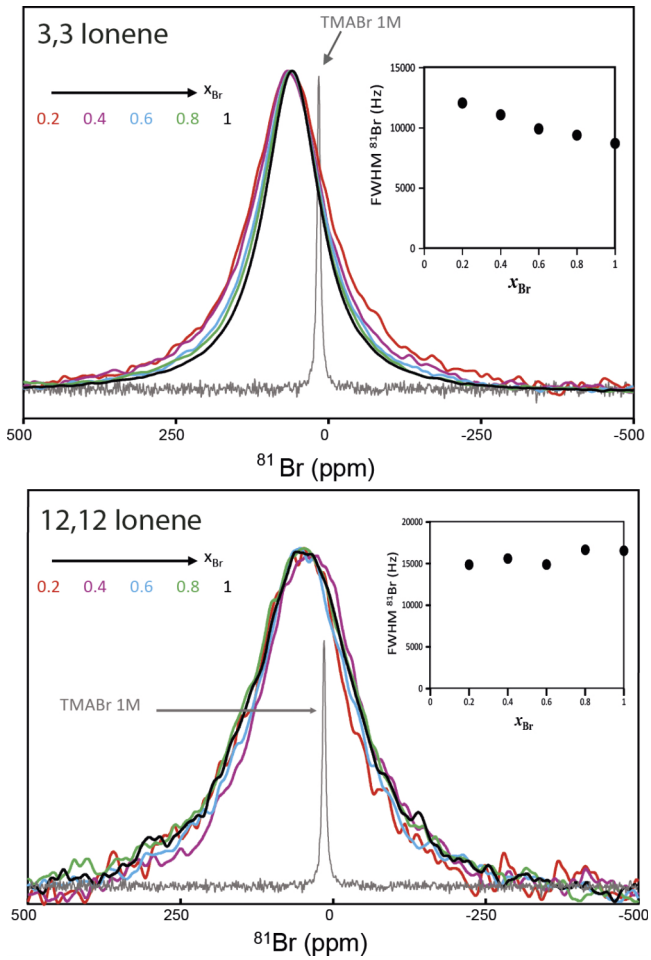

FIG. 7. ^{81}Br NMR spectra for two series of mixed Br/F ionenes: 3, 3–ionenes at $c(N^+) = 1$ M, $\phi = 0.10$ (series a, top) and 12, 12–ionenes at $c(N^+) = 0.3$ M, $\phi = 0.07$ (series c, bottom). Molar fraction of Br^- counter-ions (x_{Br}) ranges from 0.2 to 1 along each series. The insets feature the FWHM of the observed peak, plotted as a function of x_{Br}. For comparison, the ^{81}Br NMR spectrum of a 1 M TMABr solution is presented.

leads to a shift of $D(^{19}F)$ towards the reference value. The fact that data for diluted 3, 3–ionenes and 12, 12–ionenes are close in their absolute values could simply be fortuitous, we do not try to interpret this coincidence further. Never-the-less, as in the case of the chemical shift, the stronger dependence on x_{Br} is again seen only for the densely charged 3, 3–backbone, be it at high or low ionene volume fraction. This points again towards the 12,12–ionene backbone presenting a weaker perturbation for the diffusion of the F^- ions than the 3,3– backbone.

With the aim to follow the bromide-fluoride ionene–backbone binding competition also from the point of view of the more strongly binding counter-ion, Figure 7 presents ^{81}Br NMR results for the above series a (concentrated 3, 3–ionene solution) and series c (12, 12–ionene solution), again as a function of x_{Br}. In case of the ^{81}Br nucleus, it is more relevant to look at the FWHM of the NMR peak, rather than its position. As mentioned previously, ^{81}Br is a quadrupolar nucleus with a large quadrupolar constant, which leads to very high NMR relaxation rates and thus very broad spectra in comparison to ^{19}F. For comparison the ^{81}Br spectrum in a 1 M tetramethylammonium bromide (TMABr) solution is also shown. At first, it can be noticed that the FWHM is much higher in ionene systems in comparison to 1 M TMABr, it is however close to that observed for hexadecyltrimethylammonium bromide micellar systems.[47] We benefit from the meticulous study of Hedin et al.[47] on ^{81}Br relaxation for the present study on ionenes. The FWHM of the peak is directly linked to the effective NMR relaxation rate, which itself is related to the Fourier transform

of the time correlation function of the probed nucleus.[48,49] According to the relaxation models of Halle et al. applied to polyelectrolytes and micelles,[50–53] the increase of the relaxation rate of the nucleus (the counter-ion here) is associated with an increased time spent in the perturbed area, i.e. here close to the polyelectrolyte chain and in particular to the charged site. As in the case of the ^{19}F, the time-scale of the ^{81}Br NMR measurement is such that we observe an average signal over all the environments ("free" as well as "bound" states) explored by the Br^- counter-ion.

Similarly to the information from ^{19}F NMR, Figure 7 shows a clear dependence of the FWHM of the ^{81}Br peak on x_{Br} in the case of 3,3–ionene, and no such dependence for 12,12–ionene. The high charge density on the backbone is again necessary to reveal the dependence on x_{Br}. In agreement with the emerging picture, the FWHM decreases as x_{Br} increases: for small x_{Br} fractions, the majority of the Br^- counter-ions are very close to the ionene backbone, i.e. in the region of the strongest perturbation thus yielding the largest FWHM of the peak. For high x_{Br} fractions, environments both close and further away from the backbone are explored by Br^- ions leading to a narrower peak. It is interesting to note that the constant FWHM (within uncertainty) observed for 12,12–ionenes is at higher values than the series for 3,3–ionenes. This would suggest, on average, a more perturbed environment seen by the Br^- counter-ions next to 12,12–backbone. Firstly, this increased average perturbation might be related to the increasing average residence times of Br^- next to charged nitrogen centres on ionene, as we move from 3,3– to 12,12– systems. Secondly, the increased perturbation might also be linked to conformational changes of the 12,12–ionene backbone, which would affect the environment of the closely bound Br^- counter-ions. We have evidence for this based on our previous scattering data.[25] Such changes cannot be seen by the current simulations, as the length of the model chains is orders of magnitude smaller than for the real experimental systems.

The NMR data on mixed bromide-fluoride ionene solutions show overall strong differences between strongly (3,3–) and weakly (12,12–) charged ionene chains, which deserves a further comment. The charge separation on 3,3–ionenes is only 5.0 Å (increased to the Bjerrum length after Manning type condensation) and increases to 16.25 Å for 12,12–ionenes. In view of the spherical domains defined in Table III, the environment at two adjacent charged (ammonium) centers can be considered as coupled for the case of 3,3–ionenes, but independent for 12,12–ionenes. A simple picture emerges, in which the region of favorable (electrostatic) interaction for the counter-ions is a continuous "potential valley" around the 3,3–backbone, while for 12,12–backbone it is a series of distinct (spherical) sites, separated clearly by neutral regions. Within this simple picture, the local concentration of Br^- ions in the "valley" around the 3,3–backbone therefore influences the environment of an approaching F^- ion, while for a 12,12–backbone the occupancy of the adjacent sites by Br^- or F^- is irrelevant.

IV. CONCLUDING REMARKS

Thermodynamic, transport and scattering experiments revealed strong ion–specific effects in aqueous solutions of charged macromolecules. The deviations from purely electrostatic theories are large and can be, at least in part, explained by the solvation–desolvation effects, which occur in interaction between the charges in solution. This is for highly and moderately charged 3,3– and 6,6–ionenes linked to the following observations: i) Enthalpies of mixing of these ionenes with simple halide salts, ΔH_m, are mostly *negative* and decrease in the order $F^- > Cl^- > Br^- > I^-$.[17] ii) Experimental[22,23] and MD simulation data concerning the strength of counter-ion binding to the ionene oligoion arrive at the following sequence for the halide ions: F^- (weakest binding) $< Cl^- < Br^- < I^-$ (strongest binding).[26–29] The situation recently encountered with the hydrophobic 12,12–ionenes seems to differ from the above. Experimental enthalpies of mixing with simple halide salts are all *positive* this time and decrease from Br^- toward F^-, i.e. a reverse trend is seen with respect to 3,3– and 6,6–ionene solutions.[21] The current contribution focused on providing the ion-binding tendencies for 12,12–ionenes, to establish if the sequence of ions is also reversed for this property.

The most complete, though not rigorous, thermodynamic analysis of the alkali halide–ionene interaction upon mixing has been presented in Ref. 23. Bončina et al. measured ΔH_m at several

temperatures and using this information obtained the excess Gibbs free energy, enthalpy, and entropy contributions for displacement of fluoride ions in the mixing process with NaBr, NaCl, and NaI salts at T = 298 K. The results for 3,3–ionenes, shown in Table I of that paper, indicated that excess free energy function decreases in order from F^- toward I^-. The same holds true for the relevant enthalpy and entropy terms. For 6,6–ionenes the situation is slightly different. Here the decrease of the free energy relative to the solutions with fluoride ions is smaller, the same holds true for the enthalpy changes. The trends of these two quantities with respect to the type of the counter-ion are preserved; they both decrease in direction from chloride to iodide. The entropy contribution is, in contrast with the data for 3,3–ionenes, slightly positive and its trend along the sequence of anions unclear. Notice, however, that error bars in the entropy term estimates are of the order of the quantity itself.

Unfortunately, no such analysis has been performed for the most hydrophobic 12,12–ionene solutions yet. The molecular dynamics results and NMR measurements suggest that also for 12,12–ionene solutions the ion binding increases in direction from fluoride towards iodide. This finding is supported by the fact that 12,12–ionene solutions, neutralized by I^- counter-ions, are practically not soluble. The measured enthalpies of mixing, as mentioned above, are positive and they increase in the direction from NaF to NaBr. This means that also the excess entropy term caused by mixing should be positive and increase in this direction. Such a result is in contrast with the behaviour of 3,3–ionene solutions and points towards the emerging hydrophobicity of the ever longer hydrocarbon linkers between the charged centres on ionenes.[21]

MD simulations and NMR measurements presented in this work do *not* confirm the reversed trend observed for enthalpies of mixing in the case of 12,12–ionenes. The simulated results lead to the same sequence as for highly charged 3,3–ionenes and for moderately charged 6,6–ionenes. The NMR data point overall towards a lower sensitivity of the 12,12–ionene to the nature of the counter-ion, which is in line with the trend suggested by the experimental transport properties for 3,3– to 6,9– ionenes.[22]

Overall, aqueous solutions of partially hydrophobic 12,12–ionenes are clearly different from their 3,3– and 6,6–ionene analogues. They show opposite ordering of counter-ions for enthalpic measurements and for ion-binding. This should not be seen as a contradiction and can be rationalised on the basis of increasing chain hydrophobicity, which has different consequences for enthalpy and ion-binding (the latter reflecting free energy changes, with both enthalpic and entropic contributions). A signature of emerging hydrophobicity of the hydrocarbon linkers in 12,12–ionenes seems detectable through the enthalpies of dilution and mixing, and we have also reported it on the basis of neutron scattering, reflecting the effective chain-chain interactions.[25] For the ion-binding tendencies, observed here through MD and NMR, a combination of enthalpic and entropic contributions results in the same ordering observed for 12,12–ionenes and their stronger charged analogues. This situation is reminiscent of the neighbouring example of tetra-alkyl ammonium ions in aqueous solution: thermodynamic measurements clearly show increasing hydrophobicity of the ions with increasing alkyl chain length,[54] but any microscopic technique, such as neutron diffraction or MD, have never really showed a significant difference in water structuring around these ions, see for example Ref. 55.

ACKNOWLEDGMENTS

This study was supported by the Slovenian Research Agency fund (ARRS) through the Program 0103–0201, NIH USA grant GM063592. The authors thank Mojca Seručnik at the University of Ljubljana for help with sample preparation and Francois Ribot at the College de France for discussions and access to NMR spectrometers. The molecular dynamics calculations were in part performed on clusters of Ukrainian Academic Grid and the Faculty of Chemistry and Chemical Technology of the University of Ljubljana.

[1] K. D. Collins, Biophys. J. **72**, 65 (1997).
[2] R. R. Netz and D. Andelman, Phys. Rep. **380**, 1 (2003).
[3] A Y. Grosberg, T. T. Nguyen, and B. I. Shklovskii, Rev. Mod. Phys. **74**, 329 (2003).

[4] W. Kunz and R. Neueder, in *Specific Ion Effects*, edited by W. Kunz (World Scientific Publishing, Singapore, 2009), p. 11.
[5] M. A. C. Stuart, W. T. S. Huck, J. Genzer, M. Muller, C. Ober, M. Stamm, G. B. Sukhorukov, I. Szleifer, V. V. Tsukruk, M. Urban, F. Winnik, S. Zauscher, I. Luzinov, and S. Minko, Nat. Mater. **9**, 101 (2010).
[6] R. Yang, H. Wu, Y. Cao, and G. C. Bazan, J. Am. Chem. Soc. **128**, 14422 (2006).
[7] Y. Wang, B. Liu, A. Mikhailovsky, and G. C. Bazan, Adv. Mater. **22**, 656 (2010).
[8] C. Werner, *Advances in Polymer Science: Polymers for Regenerative Medicine* (Springer, Dresden, 2006).
[9] H. Noguchi, "Ionene Polymers," in *Polymeric materials encyclopedia*, edited by J. C. Salomone (CRC Press, Boca Raton, London, New York, Tokyo, 1996), p. 3392.
[10] S. Punyani and H. Singh, J. Appl. Polym. Sci. **102**, 1038 (2006).
[11] A. N. Zelikin, D. Putnam, P. Shastri, R. Langer, and V. A. Izumrudov, Bioconjugate Chem. **13**, 548 (2002).
[12] A. N. Zelikin, A. A. Litmanovich, V. V. Paraschuk, A. V. Sybatchin, and V. A. Izumrudov, Macromolecules **36**, 2066 (2003).
[13] E. S. Trukhanova, V. A. Izumrudov, A. A. Litmanovich, and A. N. Zelikin, Biomacromolecules **6**, 3198 (2005).
[14] W. Jaeger, J. Bohrisch, and A. Laschewsky, Prog. Polym. Sci. **35**, 511 (2010).
[15] J. Bachl, D. Zanuy, D. E. López-Pérez, G. Revilla-López, C. Cativiela, C. Alemán, and D. Díaz Díaz, Adv. Funct. Mater. **24**, 4893 (2014).
[16] S. Čebašek, M. Lukšič, C. Pohar, and V. Vlachy, J. Chem. Engn. Data **56**, 1282 (2011).
[17] M. Lukšič, M. Bončina, V. Vlachy, and M. Druchok, Phys. Chem. Chem. Phys. **14**, 2024 (2012).
[18] M. Seručnik, M. Bončina, M. Lukšič, and V. Vlachy, Phys. Chem. Chem. Phys. **14**, 6805 (2012).
[19] K. Arh and C. Pohar, Acta Chim. Slov. **48**, 385 (2001).
[20] M. Lukšič, B. Hribar-Lee, R. Büchner, and V. Vlachy, Phys. Chem. Chem. Phys. **11**, 10053 (2009).
[21] S. Čebašek, M. Seručnik, and V. Vlachy, J. Phys. Chem. B **117**, 3682 (2013).
[22] P. Rodič, M. Bratuša, M. Lukšič, B. Hribar–Lee, and V. Vlachy, Colloids and Surfaces A: Physicochemical and Engineering Aspects **424**, 18 (2013).
[23] M. Bončina, M. Lukšič, M. Seručnik, and V. Vlachy, Molec. Phys. **112**, 1222 (2014).
[24] N. Malikova, S. Čebašek, V. Glenisson, D. Bhowmik, G. Carrot, and V. Vlachy, Phys. Chem. Chem. Phys. **14**, 12898 (2012).
[25] N. Malikova, A.-L. Rollet, S. Čebašek, M. Tomšič, and V. Vlachy, Phys. Chem. Chem. Phys. **17**, 5650 (2015).
[26] M. Druchok, B. Hribar-Lee, H. Krienke, and V. Vlachy, Chem. Phys. Letters **450**, 281 (2008).
[27] M. Druchok, V. Vlachy, and K. A. Dill, J. Chem. Phys. **130**, 134903 (2009).
[28] M. Druchok, K. A. Dill, and V. Vlachy, J. Phys. Chem. B **113**, 14270 (2009).
[29] M. Druchok, M. Lukšič, and V. Vlachy, J. Chem. Phys. **137**, 014511 (2012).
[30] G. S. Manning, J. Chem. Phys. **51**, 924 (1969).
[31] I. Chorny, K. A. Dill, and M. P. Jacobson, J. Phys. Chem. B **109**, 24056 (2005).
[32] http://www.ccp5.ac.uk/DL_POLY_CLASSIC/.
[33] W. L. Jorgensen, D. S. Maxwell, and J. Tirado-Rives, J. Am. Chem. Soc. **118**, 11225 (1996).
[34] G. Palinkas, O. Riede, and K. Heinzinger, Z. Naturforsch. A **32**, 1197 (1977).
[35] H. J. C. Berendsen, J. R. Grigera, and T. P. Straatsma, J. Phys. Chem. **91**, 6269 (1987).
[36] S. Melchionna, G. Ciccotti, and B. L. Holian, Molec. Phys. **78**, 533 (1993).
[37] D. Wu, A. Chen, and C. S. Johnson, Jr., J. Magn. Reson. A **115**, 260 (1995).
[38] E. Fukushima and S. B. W. Roeder, *Experimental Pulse NMR* (Addison-Wesley, Reading, 1981).
[39] I. P. Gerothanassis, Prog. Nucl. Magn. Reson. Spectrosc. **19**, 267 (1987).
[40] S. Zhang, X. Wu, and M. Mehring, Chem. Phys. Lett. **173**, 481 (1990).
[41] W. Zhang and I. Furo, Biopolymers **33**, 1709 (1993).
[42] D. Massiot, F. Fayon, M. Capron, I. King, S. Le Calve, B. Alonso, J.O. Durand, B. Bujoli, Z.H. Gan, and G. Hoatson, Magn. Reson. Chem. **40**, 70 (2002).
[43] R. W. Impey, P. A. Madden, and I. R. McDonald, J. Phys. Chem. **87**, 5071 (1983).
[44] D. Laage and J. T. Hynes, J. Phys. Chem B **112**, 7697 (2008).
[45] G. Lamoureux and B. Roux, J. Phys. Chem. B **110**, 3308 (2006).
[46] U. Scheler, Curr. Opin. Colloid Interface Sci. **14**, 212 (2009).
[47] N. Hedin and I. Furo, J. Phys. Chem. B **103**, 9640 (1999).
[48] J. R. C. Van der Maarel, Concept Nucl. Magn. Reson. Part A **19A**, 97 (2003).
[49] D. E. Woessner, Concept Nucl. Magn. Reson. **13**(5), 294 (2001).
[50] B. Halle, J. Chem. Phys. **94**, 3150 (1991).
[51] B. Halle, H. Wennerström, and L. Piculell, J. Phys. Chem. **88**, 2482 (1984).
[52] B. Halle, D. Bratko, and L. Piculell, Ber. Bunsen-Ges. Phys. Chem. **89**, 1254 (1985).
[53] J. Kříž, J. Dybal, and D. Kurková, J. Phys. Chem. A **106**, 7971 (2002).
[54] Y. Marcus, J. Solution Chem. **37**, 1071 (2008).
[55] D. Bhowmik, N. Malikova, G. Mériguet, O. Bernard, J. Teixeira, and P. Turq, Phys. Chem. Chem. Phys. **16**, 13447 (2014).